Journal of Alloys and Compounds 509 (2011) 3425–3429

Contents lists available at ScienceDirect

Journal of Alloys and Compounds

journal homepage: www.elsevier.com/locate/jallcom

# Electrochemical properties of NiO/Co–P nanocomposite as anode materials for lithium ion batteries

X.H. Huang [a,*], Y.F. Yuan [b], Z. Wang [a], S.Y. Zhang [a], F. Zhou [a,*]

[a] Academy of Frontier Science, Nanjing University of Aeronautics and Astronautics, 29#, Yudao Street, Nanjing 210016, China
[b] College of Machinery and Automation, Zhejiang Sci-Tech University, Hangzhou 310018, China

ARTICLE INFO

*Article history:*
Received 25 September 2010
Received in revised form
11 December 2010
Accepted 15 December 2010
Available online 23 December 2010

*Keywords:*
NiO
Electroless cobalt plating
Composite
Anode
Lithium ion battery

ABSTRACT

NiO/Co–P nanocomposite is prepared by an electroless cobalt plating technique. The as-prepared composite is characterized by means of X-ray diffraction (XRD), energy dispersive X-ray spectroscopy (EDS), scanning electron microscopy (SEM), and transmission electron microscopy (TEM) techniques. SEM and TEM images reveal that the NiO particles are about 200 nm in size, which are modified by Co–P nanoparticles of about 30 nm. The electrochemical properties as anode materials for lithium ion batteries are examined by cyclic voltammetry (CV) and discharge–charge tests. The results show that, compared with the bare NiO without electroless cobalt plating, NiO/Co–P nanocomposite exhibits a smaller polarization and a better rate capability, which is attributed to the Co–P nanoparticles.



## 1. Introduction

3d transition-metal oxides (e.g. FeO, CoO, NiO, $Cu_2O$, and their high-valence oxides) as anode materials of lithium ion batteries have received much attention since they were first proposed by Tarascon and co-workers [1–5]. These oxides can deliver reversible capacities twice higher than carbon-based materials even at high discharge–charge current densities [6–18], and among these oxides, NiO has some advantages, e.g. stable, easy to prepare, and inexpensive. Recently, more research work on NiO anode materials focuses on how to improve their cycling stability and many methods have been developed. For example, forming composites with the conductive materials such as metals and carbon is an effective approach. These metals and carbon can remarkably improve the conductivity of active materials, facilitate the lithiation and delithiation process, and meanwhile buffer the volume changes to alleviate the pulverization of active materials [19–25].

The electroless plating is an effective method to improve the electrochemical properties of the electrode materials, because this technique readily forms a uniform metallic deposition on the surface of the materials, which is favorable to enhance their conductivity. According to the previous research [26,27], the plating Ni on the surface of the host particles is a dense film. Although this dense Ni film can improve the electronic conductivity, it may be unfavorable to the transport of lithium ions. It is believed that the granular plating materials should be more favorable for the contact between the electrolyte and active materials as well as the passing of lithium ions. Therefore, in the present work, granular cobalt plating is introduced to the surface of the NiO anode materials by electroless plating technique, and the effects of the cobalt plating on the electrochemical properties are investigated in detail.

## 2. Experimental

### 2.1. Electroless cobalt plating

Table 1 lists the compositions of the electroless cobalt plating bath. Cobalt sulfate was used as the source of cobalt, and sodium hypophosphite as the reducing agent. NiO powders, prepared by calcining the precipitation from $Ni(NO_3)_2$ and $NH_4HCO_3$ solutions, were used as the starting material. NiO powders were first pretreated by a sensitization–activation process in a mixed solution containing $SnCl_2{\cdot}2H_2O$ ($30\,g\,L^{-1}$), $PdCl_2$ ($0.5\,g\,L^{-1}$), NaCl ($160\,g\,L^{-1}$), and concentrated HCl ($60\,mL\,L^{-1}$), and subsequently transferred into the electroless cobalt plating bath with a powder load of $10\,g\,L^{-1}$. The pH value was adjusted to 10 by the addition of NaOH solution. The bath was stirred vigorously at 55 °C for 1 h. Finally, the powders were washed repeatedly with distilled water and dried at 90 °C in vacuum for 12 h.

### 2.2. Characterization of materials

The structure of the composite was characterized by X-ray diffraction (XRD, Rigaku D/max-rA with Cu Kα radiation). The component analysis of the composite was conducted using energy dispersive X-ray spectroscopy (EDS, Thermo Noran) equipped on a scanning electron microscope (SEM, FEI Sirion-100). The morpho-

* Corresponding authors. Tel.: +86 25 84893083; fax: +86 25 84893083.
*E-mail addresses:* huangxh@nuaa.edu.cn (X.H. Huang), fzhou@nuaa.edu.cn (F. Zhou).

0925-8388/$ – see front matter © 2010 Elsevier B.V. All rights reserved.
doi:10.1016/j.jallcom.2010.12.117

**Table 1**
Compositions of the electroless plating bath.

| Component | Concentration ($g\,L^{-1}$) |
|---|---|
| $CoSO_4{\cdot}7H_2O$ | 25 |
| $NaH_2PO_2{\cdot}2H_2O$ | 25 |
| $Na_3C_6H_5O_7{\cdot}2H_2O$ | 52.3 |
| $H_3BO_3$ | 25 |

logy was observed by scanning electron microscopy (SEM, Hitachi S-4800) and transmission electron microscopy (TEM, JEOL JEM200CX).

### 2.3. Electrochemical tests

NiO or NiO/Co–P nanocomposite (80 wt.%) used as the anode active materials was mixed with acetylene black (12 wt.%), and polyvinylidene fluoride (PVDF, 8 wt.%). N-methyl pyrrolidinone (NMP) was added to the mixed powders, continuously stirred until the slurry became homogeneous. The slurry was uniformly incorporated to copper foam current collector to fabricate working electrodes. The electrodes were dried at 95 °C for 12 h in vacuum and pressed under 15 MPa. Coin cells of 2025 type were assembled in an argon-filled glove box, using lithium metal foil as the counter electrode, polypropylene film as the separator, and a solution of 1 mol $L^{-1}$ $LiPF_6$ in ethylene carbonate (EC)/dimethyl carbonate (DMC) (1:1 by weight) as the electrolyte.

The cells were cyclically tested on a LAND CT2001A battery test instrument using different current densities over a voltage range of 0.02–3 V. Cyclic voltammetry (CV) tests of the electrodes were carried out on a CHI660D electrochemical workstation at a scan rate of 0.1 mV $s^{-1}$ between 0 and 3 V.

## 3. Results and discussion

### 3.1. Preparation and characterization of NiO/Co–P nanocomposite

NiO does not have self-catalysis activity for electroless cobalt plating, and needs some noble metal nanoparticles to stimulate the deposition of cobalt. Therefore, the pretreatment of sensitization–activation is necessary. If the NiO particles are not pretreated, the electroless cobalt plating does not occur at all. During the sensitization–activation process, metallic Pd nanoparticles are anchored on the surface of NiO particles and act as the nucleation centers of cobalt at the subsequent electroless plating process. This activation reaction is Eq. (1). Sodium hypophosphite is used as the reducing agent for the electroless plating because its reaction condition is milder than those of other reducing agents, e.g. hydrazine hydrate and sodium borohydride. The electroless cobalt plating reaction mainly proceeds according to Eq. (2). In addition, there are also some side reactions, including the evolution of hydrogen (Eq. (3)) and phosphorus (Eq. (4)).

$$Pd^{2+} + Sn^{2+} \rightarrow Pd + Sn^{4+} \quad (1)$$

$$Co^{2+} + H_2PO_2^- + 3OH^- \rightarrow Co + HPO_3^{2-} + 2H_2O \quad (2)$$

$$H_2PO_2^- + OH^- \rightarrow HPO_3^{2-} + H_2 \quad (3)$$

$$3H_2PO_2^- \rightarrow HPO_3^{2-} + OH^- + 2H_2O + 2P \quad (4)$$

Therefore, the use of sodium hypophosphite will introduce a small quantity of P to the deposition, leading to the formation of Co–P alloy.

EDS pattern of the NiO powders after electroless cobalt plating is shown in Fig. 1. Besides the main elements of Ni and O coming from NiO, the composite also contains 7.01 at% of Co and 1.36 at% of P. This confirms that the deposition is Co–P alloy.

Fig. 2 compares the XRD patterns of NiO before and after electroless cobalt plating. The bare NiO (pattern a) exhibits five diffraction peaks at 37.2°, 43.3°, 62.9°, 75.4°, and 79.4°, which can be assigned to the (1 1 1), (2 0 0), (2 2 0), (3 1 1), and (2 2 2) reflections of cubic NiO (JCPDS No. 47-1049). After electroless cobalt plating, besides the strong NiO reflection peaks, a broad band of weak diffraction appears at 40–50° (pattern b), which is related to the amorphous

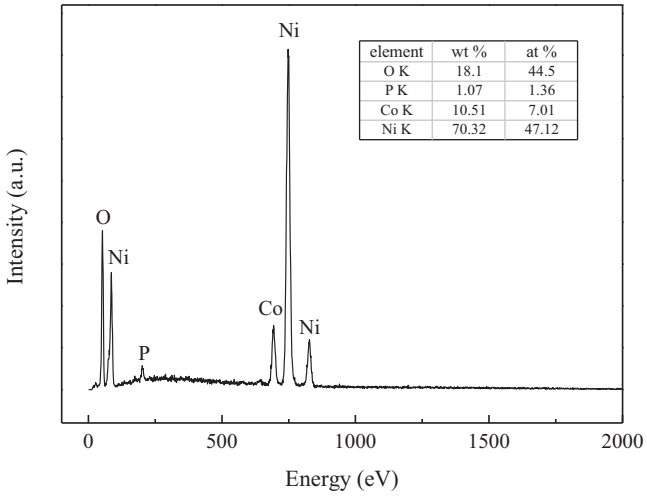


**Fig. 1.** EDS pattern of the NiO powders after electroless cobalt plating.

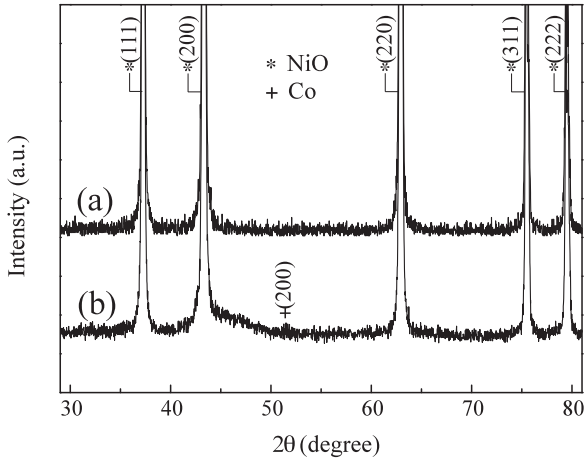


**Fig. 2.** XRD patterns of (a) bare NiO and (b) electroless cobalt-plated NiO powders.

Co–P depositions [28,29], and a weak peak at 51.5° corresponds to the (2 0 0) reflection of Co (JCPDS No. 15-0806).

Fig. 3 is the SEM image of NiO/Co–P composite. Lots of nanoparticles with the sizes of about 30 nm are uniformly deposited on the surface of the larger host particles. TEM images further show the morphology changes of NiO before and after the electroless cobalt plating (Fig. 4). The well-crystallized NiO particles are about 200 nm, and the surface is smooth (Fig. 4(a)). After the

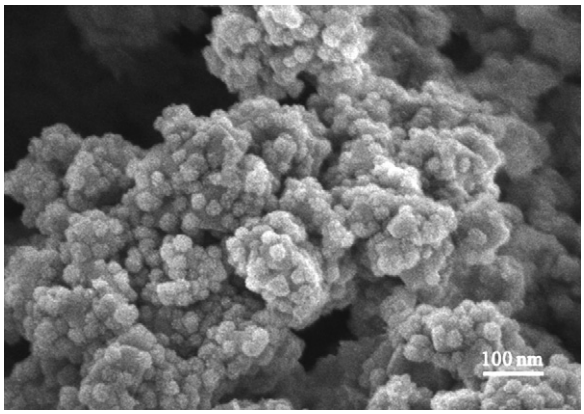


**Fig. 3.** SEM image of electroless cobalt-plated NiO.

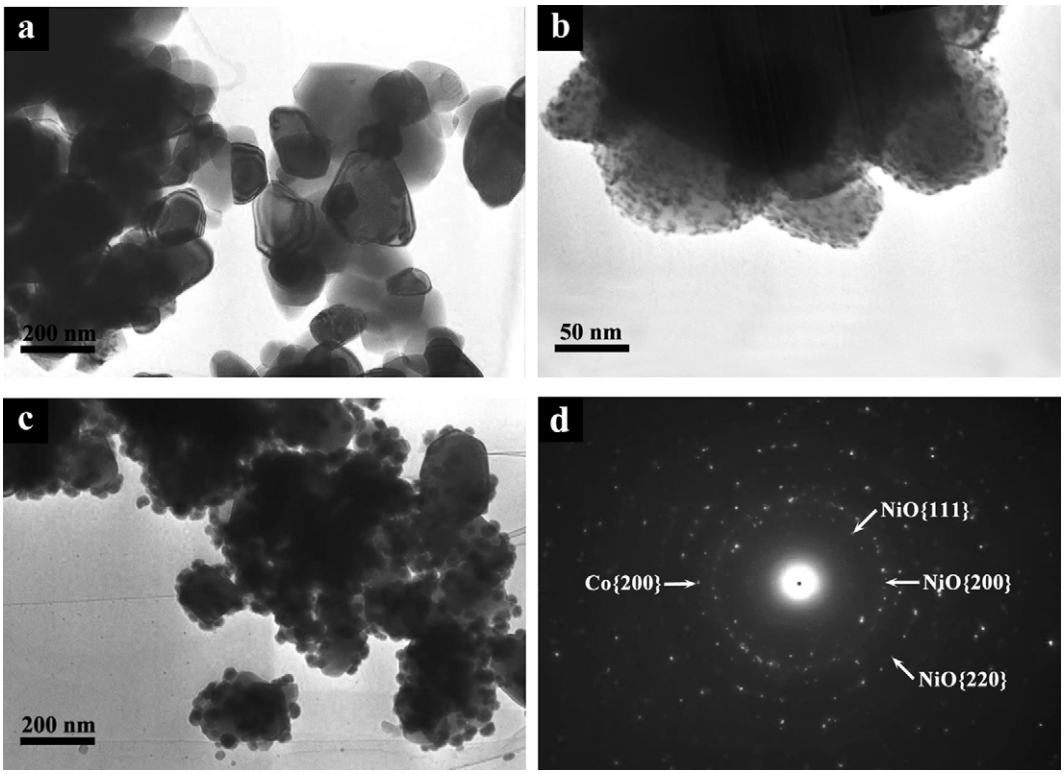


**Fig. 4.** TEM images of (a) the fresh prepared bare NiO, (b) after the sensitization and activation treatment, (c) after electroless cobalt plating, and (d) SAED pattern of NiO/Co–P nanocomposite.

sensitization–activation treatment (Fig. 4(b)), NiO are uniformly modified by numerous nanoparticles less than 10 nm. The electroless cobalt plating process makes most NiO particle entirely modified by many Co–P nanoparticles with the sizes of about 30 nm (Fig. 4(c)). Selected area electron diffraction (SAED) pattern of the electroless cobalt-plated NiO exhibits {1 1 1}, {2 0 0}, {2 2 0} reflection rings of NiO, and a {2 0 0} reflection ring of Co (Fig. 4(d)), coinciding with XRD results.

### 3.2. Electrochemical properties of NiO/Co–P nanocomposite

Electrochemical properties of the NiO/Co–P nanocomposite as anode materials for lithium ion batteries are investigated. We measure the cyclic voltammograms (CV) of NiO and NiO/Co–P between 0 and 3 V at a scan rate of 0.1 mV $s^{-1}$ (Fig. 5). The theoretical potential of the reaction ($NiO + Li \rightarrow Ni + 2Li_2O$) is 1.794 V [4], but the real reduction and oxidation peaks deviate from this value, due to polarization. For bare NiO (Fig. 5(a)), there is a strong reduction peak around 0.35 V during the first reduction scan, which is related to the first electrochemical process of the electrode. This process involves one major reaction ($NiO + 2Li \rightarrow Ni + Li_2O$), and some side reactions. The main side reaction is the formation of the gel-like solid electrolyte interphase (SEI) layer, which consists of ethylene-oxide-based oligomers, LiF, $Li_2CO_3$, and lithium alkyl carbonate ($ROCO_2Li$) [30]. Two oxidation peaks appear in the first oxidation scan. The weak one locates at about 1.55 V, which is due to the dissolution of the gel-like SEI layer during the charge process [3,5]. The main oxidation peak at about 2.25 V is stronger, and corresponds to the charge reaction ($Ni + Li_2O \rightarrow NiO + 2Li$). After the 1st cycle, the CV curves almost coincide with each other in shape, and the reduction peaks locate at 1.1 V, while the oxidation peaks locate at 1.55 and 2.25 V. This indicates that the electrode reactions become more reversible after the 1st cycle. For NiO/Co–P composite (Fig. 5(b)), the first reduction peak shifts to 0.6 V, the reversible reduction peaks shift to 1.25 V, and the main oxidation peaks shift to 2.2 V.

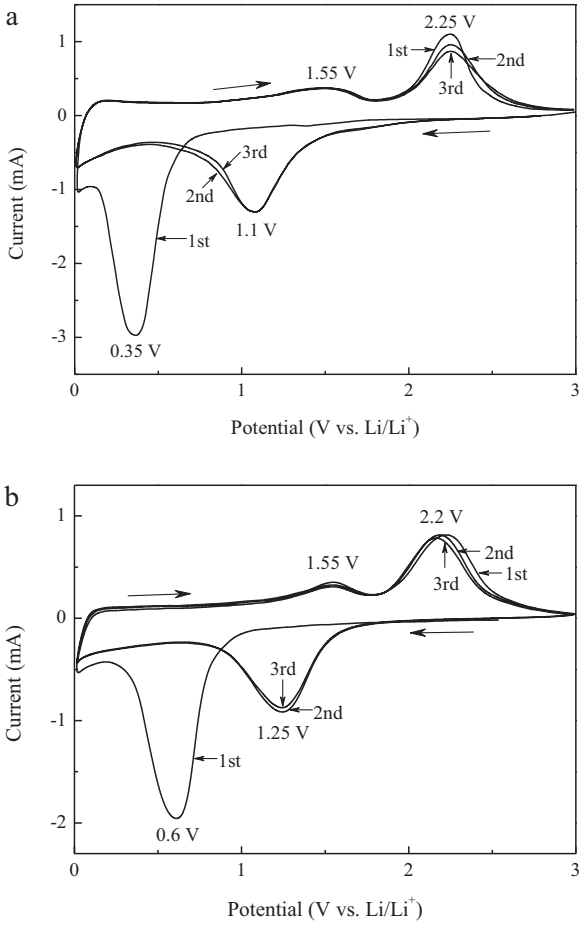


**Fig. 5.** CV curves of (a) bare NiO and (b) NiO/Co–P nanocomposite at a scan rate of 0.1 mV $s^{-1}$. The cycle numbers are marked in the graph.

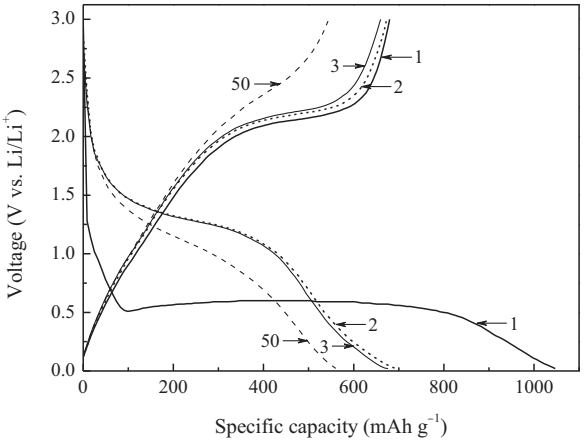


**Fig. 6.** The discharge and charge curves of the NiO/Co–P nanocomposite at a current density of 100 mA $g^{-1}$. The cycle numbers are indicated in the graph.

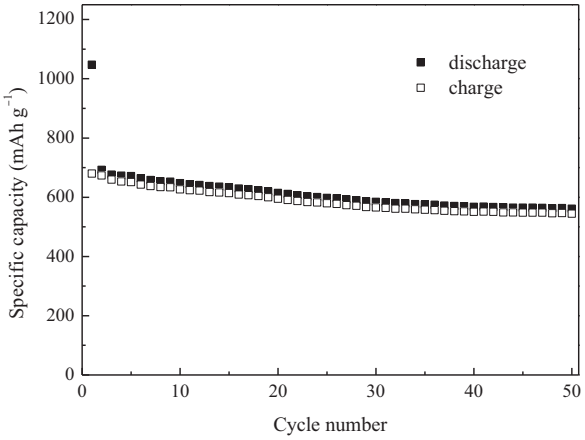


**Fig. 7.** Cycling performance of the NiO/Co–P nanocomposite at a current density of 100 mA $g^{-1}$.

Obviously, the polarization of NiO/Co–P composite is smaller than that of bare NiO, meaning that the electrode conductivity has been enhanced by electroless cobalt plating.

Fig. 6 shows the galvanostatic discharge–charge curves for the first three cycles and the 50th cycle of the NiO/Co–P composite at a current density of 100 mA $g^{-1}$. The discharge–charge plateaus all coincide well with the cathodic and anodic peaks in CV curves. An obvious long plateau located at about 0.6 V appears in the first discharge curve, but the first charge plateau is not so obvious, and the main slope is around 2.2 V. After the 1st cycle, the curves of each cycle are similar in shape, indicating that the electrode reactions become more reversible. The slope in each discharge curve is around 1.25 V, and in each charge curve is around 2.2 V, respectively. NiO/Co–P nanocomposite delivers a first discharge capacity of 1050 mAh $g^{-1}$ (determined on basis of the mass of NiO and Co–P), much higher than the theoretical value (718 mAh $g^{-1}$) of pure NiO that is calculated from the electrode reaction ($NiO + 2Li \leftrightharpoons Ni + 2Li_2O$). The extra capacity results from the irreversible side reactions including the formation of the SEI layer during the first discharge. The first charge capacity is 680 mAh $g^{-1}$, and the second discharge capacity is 690 mAh $g^{-1}$. After 50 cycles, the discharge and charge capacities remain 560 mAh $g^{-1}$ and 540 mAh $g^{-1}$, respectively. The discharge and charge capacities of the 1–50th cycles are plotted in Fig. 7. It can be seen that about 80% of the reversible capacity (charge capacity) is maintained after 50 cycles.

Co–P alloy may also react with lithium, according to Xiang et al.'s report [31], forming Co and $Li_3P$. Nevertheless, the capacity contributed by Co–P alloy nanoparticles should be very low in this work, because the content of P in the composite is only about 1 wt.%, and thus the capacity provided by $Li_3P$ is negligible.

The rate capability of NiO/Co–P nanocomposite was further evaluated as shown in Fig. 8. The bare NiO without electroless cobalt plating is also put together for a comparison. Both of the NiO and NiO/Co–P nanocomposite were tested between 0.02 and 3 V at various current densities from 100 to 1000 mA $g^{-1}$. It is obvious that NiO/Co–P nanocomposite exhibits better rate capability than bare NiO. At 100 mA $g^{-1}$, the NiO and NiO/Co–P nanocomposite exhibit similar final charge capacities, which are 635 mAh $g^{-1}$ for NiO, and 625 mAh $g^{-1}$ for NiO/Co–P nanocomposite,

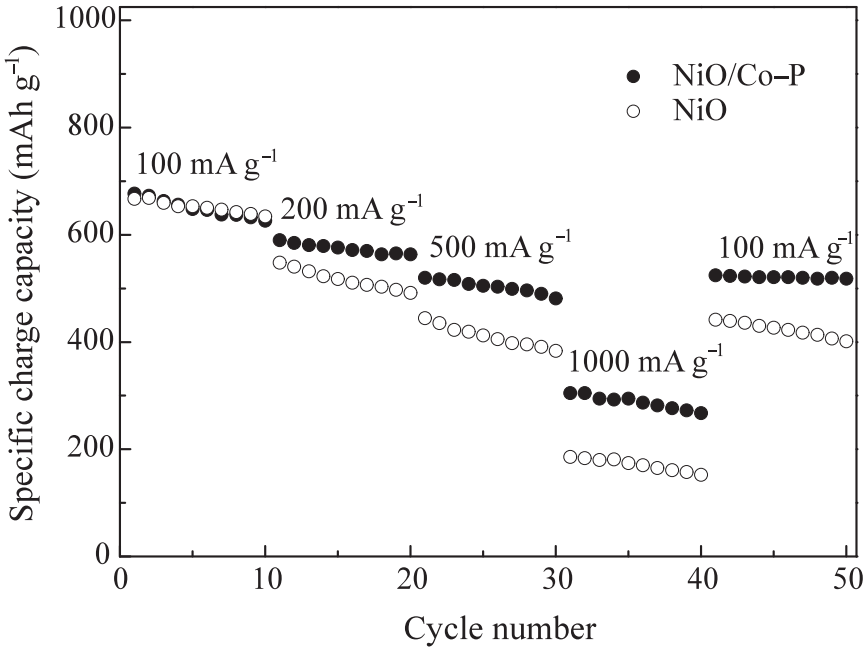


**Fig. 8.** Comparison of rate capabilities of NiO and NiO/Co–P nanocomposite.

respectively. At the higher current densities of 200 mA $g^{-1}$, 500 mA $g^{-1}$ and 1000 mA $g^{-1}$, the final charge capacities of each period for NiO are 490 mAh $g^{-1}$, 380 mAh $g^{-1}$ and 150 mAh $g^{-1}$, while for NiO/Co–P nanocomposite are up to 560 mAh $g^{-1}$, 480 mAh $g^{-1}$ and 270 mAh $g^{-1}$. When the current density returns back to the initial 100 mA $g^{-1}$, the capacities for NiO and NiO/Co–P nanocomposite can recover to 400 mAh $g^{-1}$ and 520 mAh $g^{-1}$, respectively.

Obviously, the electrochemical properties of NiO have been greatly enhanced by electroless cobalt plating. The Co–P alloy nanoparticles deposited on the surfaces of NiO particles can make the NiO particles better electrically contact each other, and offer more conductive pathways between the active materials and the current collector. As a result, the electrochemical reactions of the active materials can proceed more quickly and completely, leading to the higher capacity and enhanced rate capability. Meanwhile, the Co–P alloy nanoparticles can also buffer the volume changes and alleviate the pulverization of the NiO particles, which is beneficial to the electrochemical properties.

## 4. Conclusions

NiO/Co–P nanocomposite has been successfully prepared by an electroless cobalt plating technique. Co–P alloy nanoparticles, with an average size of 30 nm, are deposited on the surfaces of the NiO particles. Electrochemical tests show that the nanocomposite delivers discharge and charge capacities of 560 mAh $g^{-1}$ and 540 mAh $g^{-1}$ after 50 cycles at the current density of 100 mA $g^{-1}$, and also exhibit smaller polarization and better rate capability than bare NiO. The Co–P nanoparticles in the composite can improve the conductivity of the electrode materials, and is able to tolerate the volume change of the active particles. The two aspects lead to the improvement of the electrochemical properties.

## Acknowledgements

This work is supported by China Postdoctoral Science Foundation (no. 20090461109), Jiangsu Postdoctoral Science Research Foundation (no. 0902015C), and Science Foundation of Nanjing University of Aeronautics and Astronautics (no. 909388). We would like to acknowledge them for financial support.

## References

[1] P. Poizot, S. Laruelle, S. Dupont, J.-M. Tarascon, Nature 407 (2000) 496–499.
[2] J.-M. Tarascon, M. Armand, Nature 414 (2001) 359–367.
[3] S. Grugeon, S. Laruelle, R. Herrera-Urbina, L. Dupont, P. Poizot, J.-M. Trarscon, J. Electrochem. Soc. 148 (2001) A285–A292.
[4] P. Poizot, S. Laruelle, S. Grugeon, J.-M. Tarascon, J. Electrochem. Soc. 149 (2002) A1212–A1217.
[5] A. Débart, L. Dupont, P. Poizot, J.-B. Leriche, J.M. Tarascon, J. Electrochem. Soc. 148 (2001) A1266–A1274.
[6] Y. Sun, X.Y. Feng, C.H. Chen, J. Power Sources 196 (2011) 784–787.
[7] Y. Lu, Y. Wang, Y. Zou, Z. Jiao, B. Zhao, Y. He, M. Wu, Electrochem. Commun. 12 (2010) 101–105.
[8] J. Jiang, J. Liu, R. Ding, X. Ji, Y. Hu, X. Li, A. Hu, F. Wu, Z. Zhu, X. Huang, J. Phys. Chem. C 114 (2010) 929–932.
[9] J.C. Park, J. Kim, H. Kwon, H. Song, Adv. Mater. 21 (2009) 803–807.
[10] P. Zhang, Z.P. Guo, H.K. Liu, Electrochim. Acta 55 (2010) 8521–8526.
[11] J. Ma, S. Zhang, W. Liu, Y. Zhao, J. Alloys Compd. 490 (2010) 647–651.
[12] S. Gurmen, B. Ebin, J. Alloys Compd. 492 (2010) 585–589.
[13] H. Wang, Q. Pan, J. Zhao, W. Chen, J. Alloys Compd. 476 (2009) 408–413.
[14] H. Liu, D. Wexler, G. Wang, J. Alloys Compd. 487 (2009) L24–L27.
[15] Q. Pan, K. Huang, S. Ni, F. Yang, S. Lin, D. He, J. Alloys Compd. 484 (2009) 322–326.
[16] J.Y. Xiang, J.P. Tu, L. Zhang, Y. Zhou, X.L. Wang, S.J. Shi, J. Power Sources 195 (2010) 313–319.
[17] J.Y. Xiang, J.P. Tu, J. Zhang, J. Zhong, D. Zhang, J.P. Cheng, Electrochem. Commun. 12 (2010) 1103–1107.
[18] X.H. Huang, J.P. Tu, X.H. Xia, X.L. Wang, J.Y. Xiang, L. Zhang, Y. Zhou, J. Power Sources 188 (2009) 588–591.
[19] Q. Pan, L. Qin, J. Liu, H. Wang, Electrochim. Acta 55 (2010) 5780–5785.
[20] M. Gao, X. Chen, H. Pan, L. Xiang, F. Wu, Y. Liu, Electrochim. Acta 55 (2010) 9067–9074.
[21] J. Kim, M.K. Chung, B.H. Ka, J.H. Ku, S. Park, J. Ryu, S.M. Oh, J. Electrochem. Soc. 157 (2010) A412–A417.
[22] C. Feng, L. Li, Z. Guo, H. Li, J. Alloys Compd. 504 (2010) 457–461.
[23] J. Wang, X.M. Liu, H. Yang, X.D. Shen, J. Alloys Compd. 509 (2011) 712–718.
[24] H. Zhang, H. Tao, Y. Jiang, Z. Jiao, M. Wu, B. Zhao, J. Power Sources 195 (2010) 2950–2955.
[25] Y. He, L. Huang, J.S. Cai, X.M. Zheng, S.G. Sun, Electrochim. Acta 55 (2010) 1140–1144.
[26] Y.F. Yuan, J.P. Tu, S.Y. Guo, J.B. Wu, M. Ma, J.L. Yang, X.L. Wang, Appl. Surf. Sci. 254 (2008) 5080–5084.
[27] C.Q. Zhang, J.P. Tu, Y.F. Yuan, X.H. Huang, X.T. Chen, F. Mao, J. Electrochem. Soc. 154 (2007) A65–A69.
[28] C. Zhang, G.P. Ling, J.H. He, Mater. Lett. 58 (2003) 200–204.
[29] J.T. Jiang, L. Zhen, L. Yang, W.Z. Shao, C.Y. Xu, Z.M. Chao, Surf. Coat. Technol. 203 (2009) 2221–2228.
[30] G. Gachot, S. Grugeon, M. Armand, S. Pilard, P. Guenot, J.-M. Tarascon, S. Laruelle, J. Power Sources 178 (2008) 409–421.
[31] J.Y. Xiang, X.L. Wang, X.H. Xia, J. Zhong, J.P. Tu, J. Alloys Compd. 509 (2011) 157–160.